AJNR

MR of pediatric intracranial meningiomas.

C F Darling, S E Byrd, M Reyes-Mugica, T Tomita, R E Osborn, M A Radkowski and E D Allen

AJNR Am J Neuroradiol 1994, 15 (3) 435-444
http://www.ajnr.org/content/15/3/435

MR of Pediatric Intracranial Meningiomas

Crystal F. Darling, Sharon E. Byrd, Miguel Reyes-Mugica, Tadanori Tomita, Robin E. Osborn, Mary Ann Radkowski, and Evan D. Allen

PURPOSE: To assess MR and pathologic characteristics of childhood intracranial meningiomas, comparing the radiographic findings with those observed in adult intracranial meningiomas. **METHODS:** Clinical records, MR and CT scans, and histology of eight children with intracranial meningiomas presenting for a period of 7.5 years were retrospectively reviewed. **RESULTS:** Boys equaled girls but predominated from ages 4 to 11 years. The ages ranged from 4 to 18 years. Two patients had radiation-induced meningiomas. Two children had multiple lesions; neither had neurofibromatosis. All solitary lesions were supratentorial. Other characteristics included: dural-based attachment (n = 6); large size (>5 cm) (n = 4); cystic components (n = 3); and intraventricular location (n = 1). Histologic subtypes were: meningothelial (n = 4); transitional (n = 3); and fibroblastic (n = 1). Preoperative diagnoses of meningiomas were made in six cases based on overall imaging characteristics. **CONCLUSIONS:** Diagnosis of childhood intracranial meningiomas does not differ from that of adults radiographically, with the exception of larger tumor sizes.

Index terms: Meninges, magnetic resonance; Meninges, neoplasms; Neoplasms, in infants and children

AJNR Am J Neuroradiol 15:435–444, Mar 1994

Intracranial meningiomas are common in adults and rare in children. Meningiomas account for 1.4% to 4% of pediatric intracranial neoplasms (1). Meningiomas occurring in children are considered to differ significantly from their adult counterparts by having larger size; higher frequency of cystic changes, absence of dural based attachment, and intraventricular location; more aggressive/malignant nature; male predominance; and higher incidence of multiplicity associated with neurofibromatosis (1–4).

In this retrospective study to review the imaging characteristics of meningiomas occurring in our pediatric patients, we investigated: 1) magnetic resonance (MR) findings and correlation with histologic subtypes; 2) differences between computed tomography (CT) and MR in diagnosing and evaluating meningiomas; and 3) the patient population in the medical literature for comparison with ours.

Received October 25, 1991; accepted pending revision December 12; revision received April 7, 1993.

From the Division of Neuroimaging, Department of Radiology (C.F.D., S.E.B., R.E.O., M.A.R., E.D.A.), the Department of Pathology (M.R.-M.), and the Division of Neurosurgery, Department of Surgery (T.T.), Children's Memorial Hospital and Northwestern Medical School, Chicago, Ill.

Address reprint requests to Sharon E. Byrd, MD, Division of Neuroimaging, Children's Memorial Hospital, 2300 Children's Plaza, Chicago, IL 60614.

AJNR 15:435–444, Mar 1994 0195-6108/94/1503–0435

Materials and Methods

The MR and CT images of eight children with surgically and histologically proved meningiomas presenting over the past 7.5 years were retrospectively reviewed. Children 18 years and younger are included as pediatric patients at our institution. The ages of the children in our series ranged from 4 to 18 years (11.4 years mean). There were four boys and four girls. Seven children were scanned on a 1.5-T MR unit; one child was imaged on a low-field-strength (0.5-T) scanner. Using a 5-mm section thickness, 1-mm intersection gap, and 256 × 192 matrix, all patients were imaged with spin-echo 600/20/2 (repetition time/echo time/excitations) and spin-echo 2000/30–80/2 pulse sequences in the axial plane. Additional T1-weighted images in the sagittal, axial, and coronal projections were obtained. Gadolinium was injected intravenously at 0.2 mL/kg with a maximum dose of 20 mL.

Seven children also had CT scans. These studies were performed before and after intravenous contrast (iohexol 300) infusion at 2–4 mL/kg, a maximum dose of 150 mL. Section thicknesses were obtained as 5-mm contiguous sections.

Results

Table 1 is a summary of the clinical and pathologic findings of our eight children with intracranial meningiomas.

Clinical

Although there was an equal number of boys and girls in our series, of the five children presenting between 4 and 11 years of age, there was a distinct male predominance of 4.

The majority of children (n = 7) presented with signs and/or symptoms of increased intracranial pressure (nausea, vomiting, headache, and papilledema). One child had a right homonomous hemianopsia. Another child presented with an isolated third cranial nerve palsy. None of the patients had the stigmata or diagnosis of neurofibromatosis.

A significant medical history was obtained in two cases. Both children were girls who had been treated 13 and 15 years earlier for acute lymphocytic leukemia. They had been treated with high-dose external beam radiation and chemotherapy to the central nervous system.

Surgical Pathology

All of the children underwent surgical exploration with either complete or partial resection of their tumors. Each specimen had gross and microscopic analysis. The classification used by our pathologist was based on the modified World

TABLE 1: Childhood intracranial meningiomas: clinical and pathologic findings

Case	Age (years)	Sex	Clinical Presentation	Pertinent History	Pathology	Location	Size (cm)
1 (Z.E.)	8	F	Headaches, nausea, vomiting, photophobia, papilledema, right homonymous hemianopsia		Transitional (mixed) meningotheliomatous and fibrous; non-dural–based	Left lateral ventricle	8 × 7 × 6
2 (M.R.)	11	M	Headaches, head turning to left, papilledema		Fibrous; 80% sclerosed	Right lateral posterior temporoparieto-occipital	7 × 8 × 7
3 (F.K.)	18	F	Headaches	Treated for acute lymphoblastic leukemia 15 years before with whole brain radiation and chemotherapy	Meningotheliomatous	Left lateral sphenoid wing/pterion	3 × 3 × 4
4 (F.D.)	16	F	Headaches, blurred vision, papilledema	Treated for acute leukemia 13 years before with chemotherapy and craniospinal radiation	Meningotheliomatous with necrosis and prominent fibrous septations; cystic	Right frontoparietal	8 × 8 × 6
5 (E.S.)	8	M	Headaches		Transitional (mixed) meningotheliomatous and fibrous; non-dural–based	Left sylvian fissure	2 × 2 × 2
6 (M.R.)	4	M	Third nerve palsy		Meningotheliomatous with abundant psammoma bodies; cystic components	1. Right medial orbit	1 × 1 × 1
						2. Right olfactory tract	1 × 1 × 1
						3. Right cavernous sinus	1 × 1 × 1
7 (W.K.)	9	M	Headaches, nausea, vomiting		Meningotheliomatous	Right sphenoid wing, middle cranial fossa and frontotemporal	10 × 7 × 8
8 (K.A.)	17	F	Headaches, papilledema		Transitional (mixed) meningotheliomatous and fibrous; cystic components	1. Parasagittal frontal	2 × 3 × 1
						2. Parasagittal left parietal	4 × 2 × 5
						3. Posterior fossa	2 × 1 × 1

Note.—Pathology is based on modified classification of the World Health Organization (2).

Health Organization classification, which incorporates biochemical and cell receptor studies with traditional histologic examination (2). The histology of the meningiomas fell into three basic subtypes: meningothelial (n = 4); transitional (n = 3); and, fibroblastic (n = 1) (Fig 1). No malignant or angioblastic meningiomas were found in our series. Six children had dural-based meningiomas; two tumors were nondural based.

Imaging

Meningiomas 1 cm or less were considered small; between 1 and 5 cm, moderate; and greater than 5 cm, large. In our eight cases, a total of 12 lesions were found. Four of the children had large meningiomas, the average size being 8 cm. Five of the lesions were moderate in size, and three were small.

Two children presented with multiple intracranial meningiomas (Fig 2). Both children had three intracranial tumors each.

Cystic components were found in three of the meningiomas. None of the cysts was larger than the solid component of the tumor (Fig 3). The cysts were small, ranging from 10% to 30% of the total size of the meningioma. The cystic portions on all MR pulse sequences showed signal intensity identical to cerebrospinal fluid (CSF).

The location of the meningiomas in our children was mainly at the level of the middle cranial fossa. These tumors arose from the floor, greater sphenoid wing, pterion, or lateral midconvexity of the temporal or parietal regions. Two of the patients had meningiomas that arose from nondural–based locations: one was an intraventricular meningioma; the other arose from deep within the sylvian fissure (Figs 4 and 5).

The signal intensities of the solid portions of the subtypes of meningiomas in our patients corresponded to Elster et al's data on histopathologic MR intensity (3). Meningotheliomatous (4) and transitional (2) meningiomas demonstrated isointensity to gray matter and hypointensity to

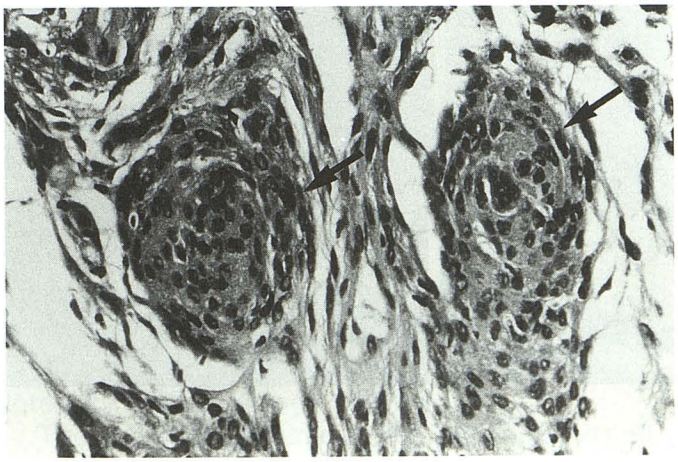

A

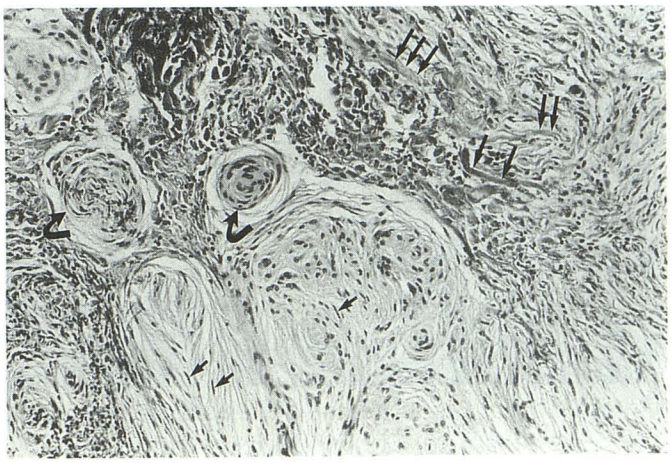

B

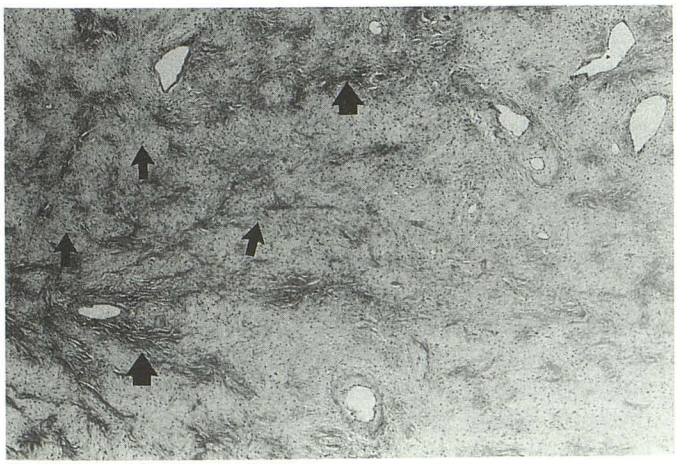

C

Fig. 1. Histopathologic findings.

A, Whorling cell pattern (*arrows*) characteristic of meningothelial differentiation (Table 1, case 7). Hematoxylin and eosin stain, magnification 250×.

B, Spindle elements (*short arrows*) intermingle with whorling cellular structures (*curved arrows*) and abundant collagen fibers (*long arrows*) seen in transitional meningioma (Table 1, case 1). Hematoxylin and eosin stain, magnification 160×.

C, Fibrous meningioma showing spindle cell morphology (*thin arrows*) and prominent sclerosis (*thick arrows*) (Table 1, case 2). Hematoxylin and eosin stain, magnification 25×.

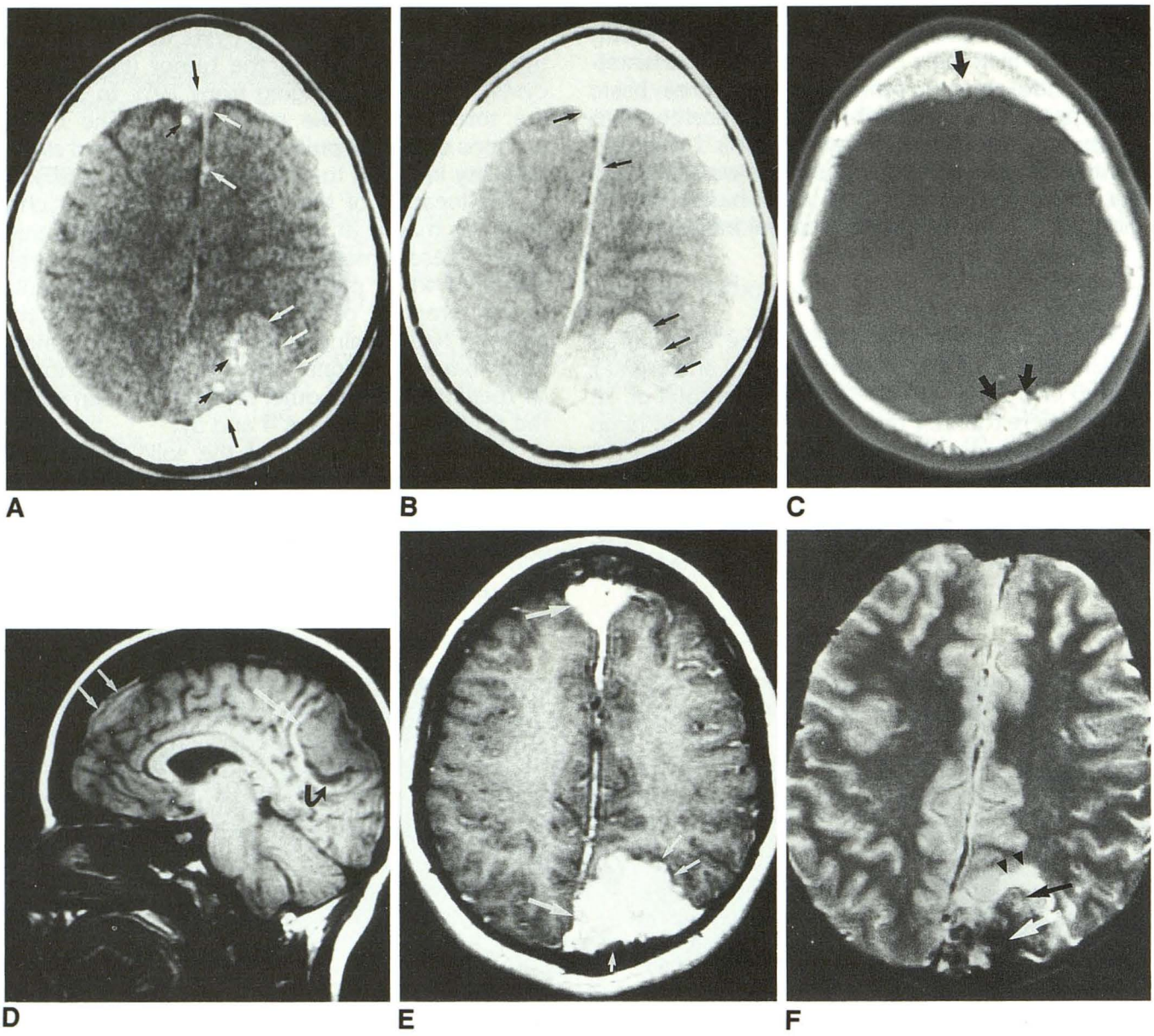

Fig. 2. Multiple mixed meningiomas (Table 1, case 8).

A, Axial noncontrast CT demonstrates multiple dense meningiomas (*white arrows*) with foci of calcifications (*short black arrows*) and calvarial bony hyperostosis (*long black arrows*).

B, Axial contrast-enhanced CT shows dense tumor enhancement (*arrows*).

C, Bone window settings (window = 550, level = 2100) better demonstrate hyperostosis (*arrows*).

D, Sagittal T1-weighted MR shows isointense to gray matter, parasagittal meningiomas which are in the frontal (*small arrows*) and posterior parietal (*large arrow*) lobes. The latter has a CSF interface (*curved arrow*).

E, Axial T1-weighted postcontrast image shows marked tumor enhancement (*large arrows*), CSF interface (*small arrows*) and hyperostosis (*short arrow*).

F, Axial T2-weighted image shows the tumor to be isointense to gray matter (*black arrow*), with hypointense calcifications (*white arrow*) and a small rim of edema (*arrowheads*).

white matter on T1-weighted images. There was isointensity to gray matter and slight hyperintensity to white matter on T2-weighted (Figs 2 and 3). A third case of transitional meningioma demonstrated mixed signal intensity on both T1-weighted and T2-weighted images, secondary to abundant calcium within the tumor (Fig 4). The single case of fibroblastic meningioma had an unusual signal intensity on MR. On T1-weighted images, it appeared isointense to gray matter and

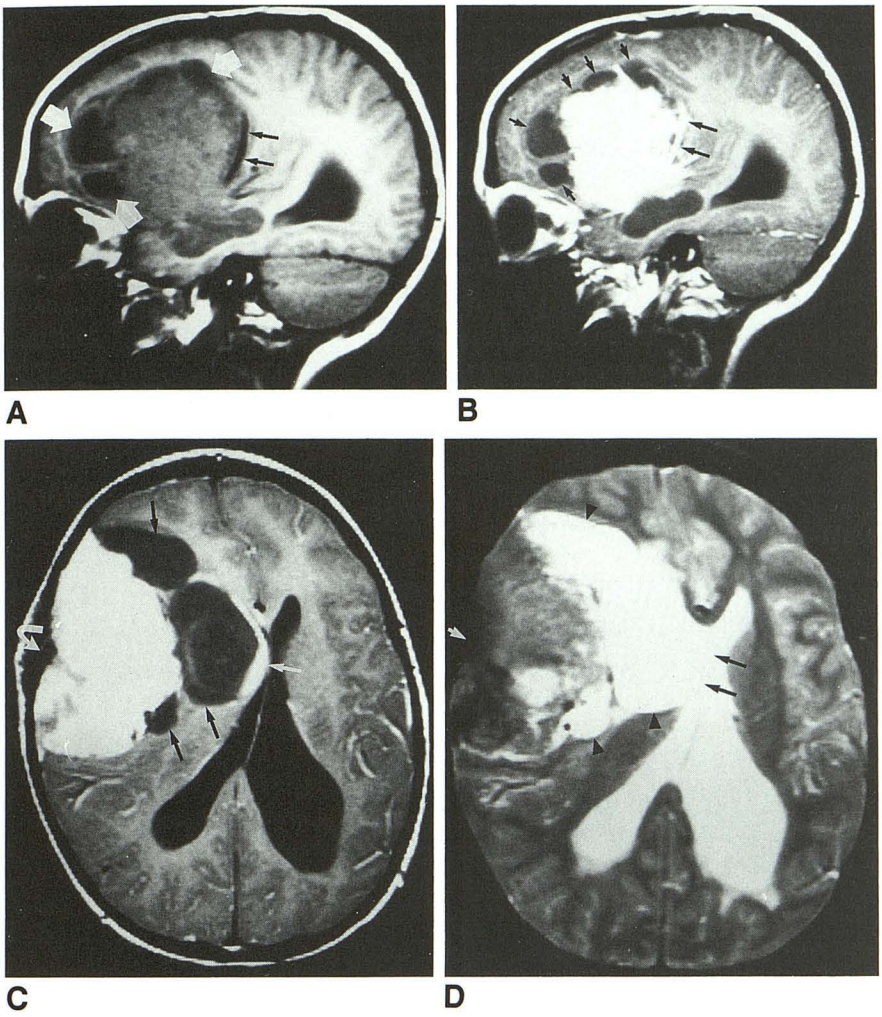

Fig. 3. Cystic meningotheliomatous meningioma (Table 1, case 4).

A, Sagittal T1-weighted MR of a right frontoparietal meningioma which is isointense to hypointense to gray matter. There are peripheral cysts (*white arrows*) and a vascular interface (*black arrows*).

B, Sagittal T1-weighted postcontrast image shows markedly homogenous tumor and vascular interface (*long arrows*) enhancement. The cysts remain unenhanced (*short arrows*).

C, Axial T1-weighted postcontrast image with vascular interface enhancement (*white arrow*), peripheral cysts (*black arrows*), and hyperostosis (*curved arrow*).

D, Axial T2-weighted image demonstrates heterogenous tumor signal intensity with low signal hyperostosis (*white arrow*). The cysts (*arrowheads*) are isointense to CSF. The vascular interface (*black arrows*) demonstrates increased venous signal intensity which can be seen on gated T2-weighted images.

hypointense to white matter. On T2-weighted images, it was markedly hypointense centrally to both gray and white matter and of mixed signal intensity peripherally (Fig 6).

The solid components of the meningiomas all enhanced markedly after gadolinium was administered. With the exception of the intraventricular meningioma, an interface could be delineated between the brain and the tumor on MR.

Calcium was difficult to evaluate on MR even when CT clearly showed areas of calcification within a tumor (Figs 2, 4–6). This occurred in six of the eight cases. Calcifications were large and easily demonstrable in one case on both MR and CT. In another lesion, microcalcifications were identified on histologic examination.

We did not find any evidence of hemorrhage, fat, or tumor necrosis within the neoplasms on MR. There were false-positive and false-negative readings of tumoral necrosis. One tumor showed a central area of hypointensity to gray matter on T1-weighted images before and after gadolinium but also marked hypointensity on T2-weighted images. This region did not follow CSF intensity patterns to suggest cystic change (Fig 6). We felt that this represented an area of tumor necrosis. Pathologic analysis revealed no areas of necrosis but instead a region of total fibrosis with 80% sclerosis. A second tumor demonstrated diffuse homogenous enhancement on both CT and MR with no areas of low density on CT or hyposignal intensity on MR precontrast studies. Microscopic examination demonstrated definite areas of necrosis.

There was no correlation between the amount of peritumoral edema and the size or histologic subtype of meningioma. The edema was graded as mild if it extended less than 1 cm from the periphery of the tumor, moderate if it extended 1 to 4 cm, and severe if larger than 4 cm. Severe edema occurred only in the one intraventricular

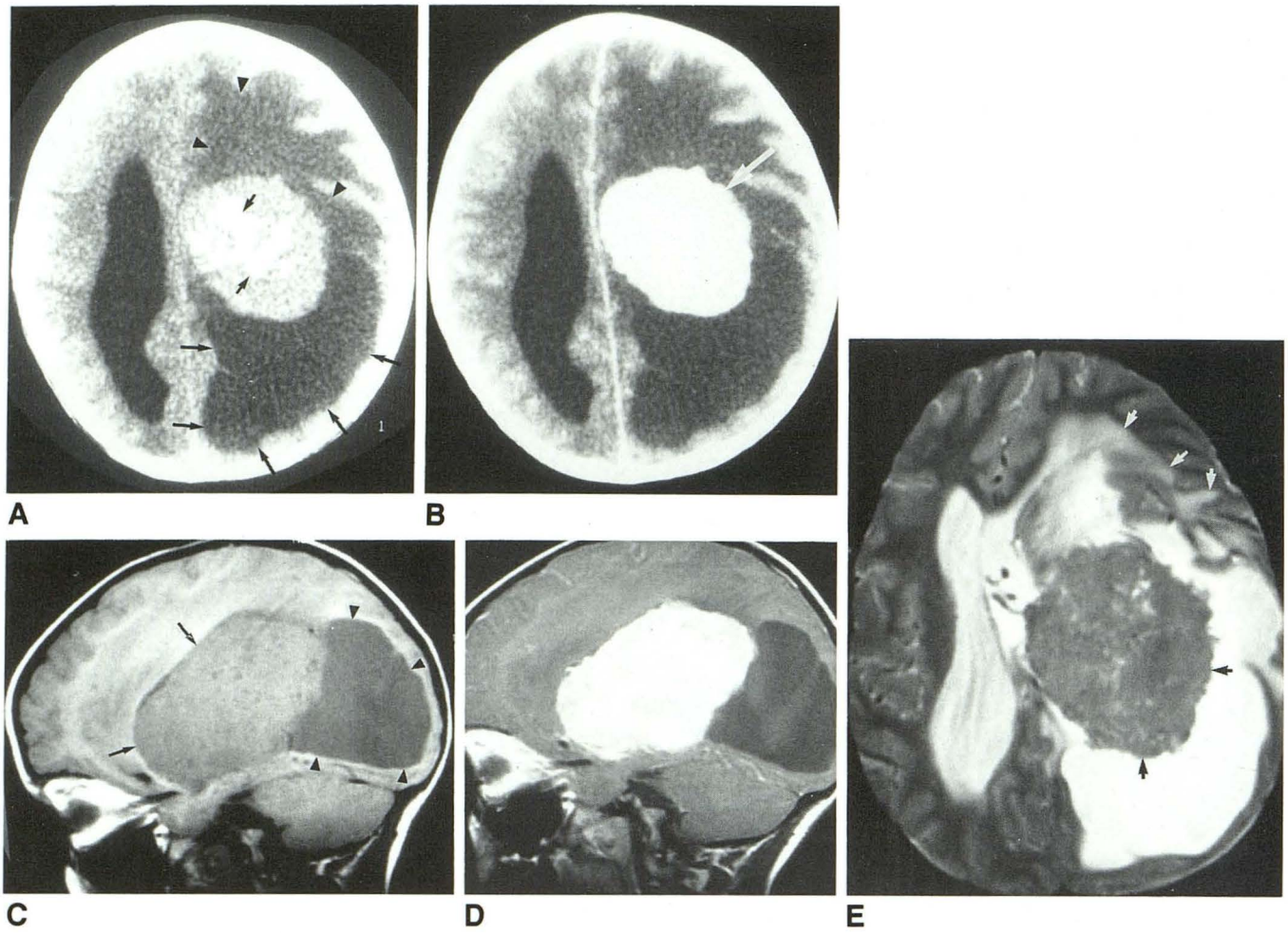

Fig. 4. Intraventricular mixed meningioma (Table 1, case 1).

A, Axial noncontrast CT shows left lateral intraventricular meningioma with central large mottled calcifications (*small black arrows*), dilated ventricle (*large black arrows*) and edema (*arrowheads*).

B, Axial contrast-enhanced CT shows marked homogenous tumor enhancement (*arrow*).

C, Sagittal T1-weighted MR shows tumor isointense to gray matter (*arrows*) within the dilated lateral ventricle (*arrowheads*).

D, Sagittal T1-weighted postcontrast image with heterogenous meningioma enhancement.

E, Axial T2-weighted image shows heterogeneous signal intensity of the tumor (*black arrows*) and surrounding edema (*white arrows*).

meningioma. Edema was best evaluated on T2-weighted images (Figs 4 and 6).

The degree of hydrocephalus correlated best with the size of the neoplasm and was graded subjectively as mild, moderate, or severe. Three of the large meningiomas caused moderate hydrocephalus, and one large meningioma caused mild hydrocephalus. Three of the children with moderate-sized lesions and the one with small tumors had no hydrocephalus.

The CT findings of the meningiomas in our children correlated quite well with those described in the literature (1, 4, 7). The solid parts of the meningiomas were denser than the cortical gray matter before contrast and enhanced diffusely and homogeneously after contrast in a pattern similar to that seen on MR. Calcifications were better identified on noncontrast CT as were the bony changes of hyperostosis and calvarial thinning. Hyperostosis can be demonstrated on MR as low signal intensity of thickening on T1-weighted and T2-weighted images (Fig 2).

Discussion

Because pediatric intracranial meningiomas are rare, the MR characteristics have not been well delineated in the radiology literature. Our series of eight intracranial meningiomas presenting over a 7.5-year period, with seven children presenting

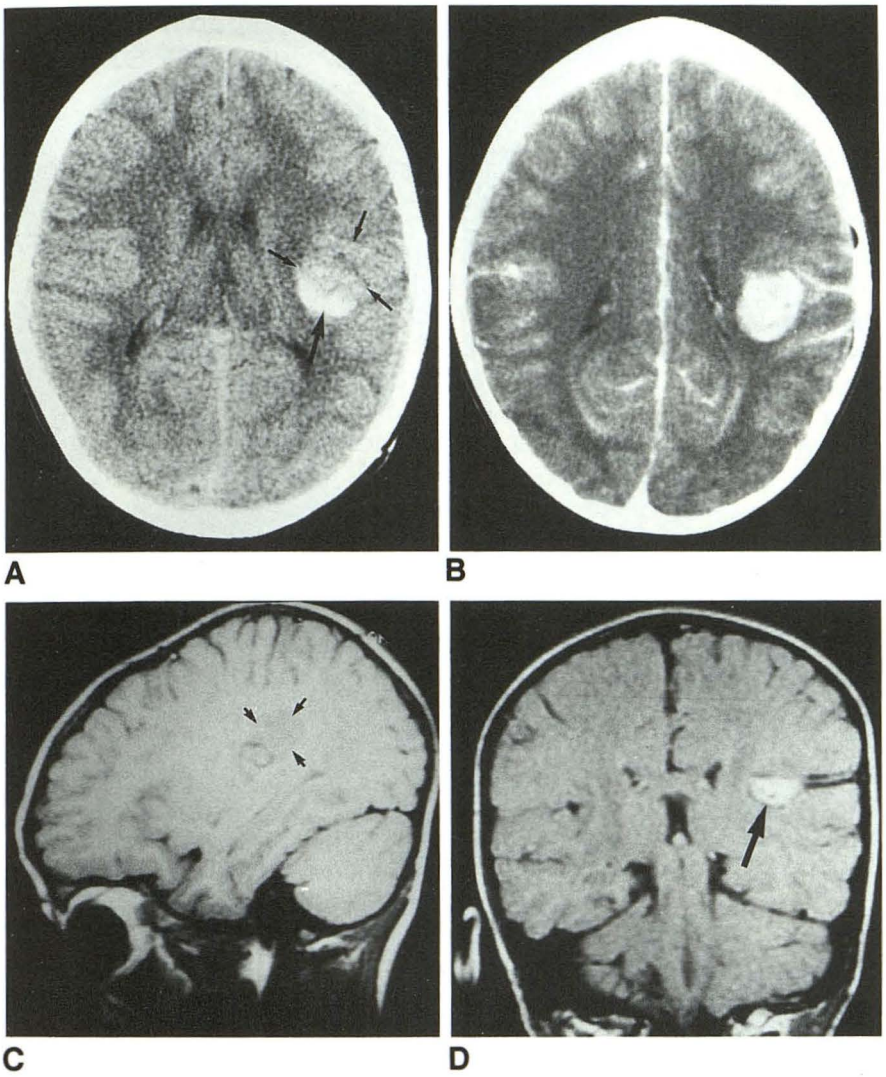

Fig. 5. Sylvian fissure mixed meningioma (Table 1, case 5).

A, Axial noncontrast CT demonstrates a small lesion within the left sylvian fissure which is isodense to gray matter (*small arrows*). Coarse calcifications (*large arrow*) are also identified.

B, Axial contrast-enhanced CT shows marked homogenous tumor enhancement.

C, Sagittal T1-weighted image shows the meningioma within the superior aspect of the sylvian fissure (*arrows*).

D, Coronal T1-weighted postcontrast image clearly shows the location and marked homogenous tumor enhancement (*arrows*).

within a 3-year period, seems to be small. However, it is fairly large in comparison with other studies over a given time frame: 19 from 1952 to 1987; 13 over a 51-year period; 4 from 1960 to 1981; and 22 from 1970 to 1987 (4–7). We have given a detailed review of the characteristics of these neoplasms and compared our findings with those reported previously.

Clinical

In the literature, there is a male predominance in children with intracranial meningiomas under the age of 16 years (1). There was an equal number of girls and boys in our group of eight children; however, of the five children presenting between 4 and 11 years of age, there was a male predominance of four boys.

Signs and symptoms of raised intracranial pressure (23% to 70%), focal neurologic deficits (40% to 46%), and seizures (10% to 23%) are the most common findings in children with intracranial meningiomas (4, 5). Again, the clinical manifestations presenting in the children in our series were similar to those found in the literature. Seven patients had signs and symptoms related to raised intracranial pressure, and two of the children presented with focal neurologic deficits.

There are reports cited in the literature of up to 19% of adolescents with meningiomas also having neurofibromatosis type 2. Multiple meningiomas are considered rare in children with a frequency of 2.5% but more common when associated with neurofibromatosis type 2 (8). Neither of our two cases of multiple meningiomas had any of the physical or imaging findings to warrant the diagnosis of neurofibromatosis.

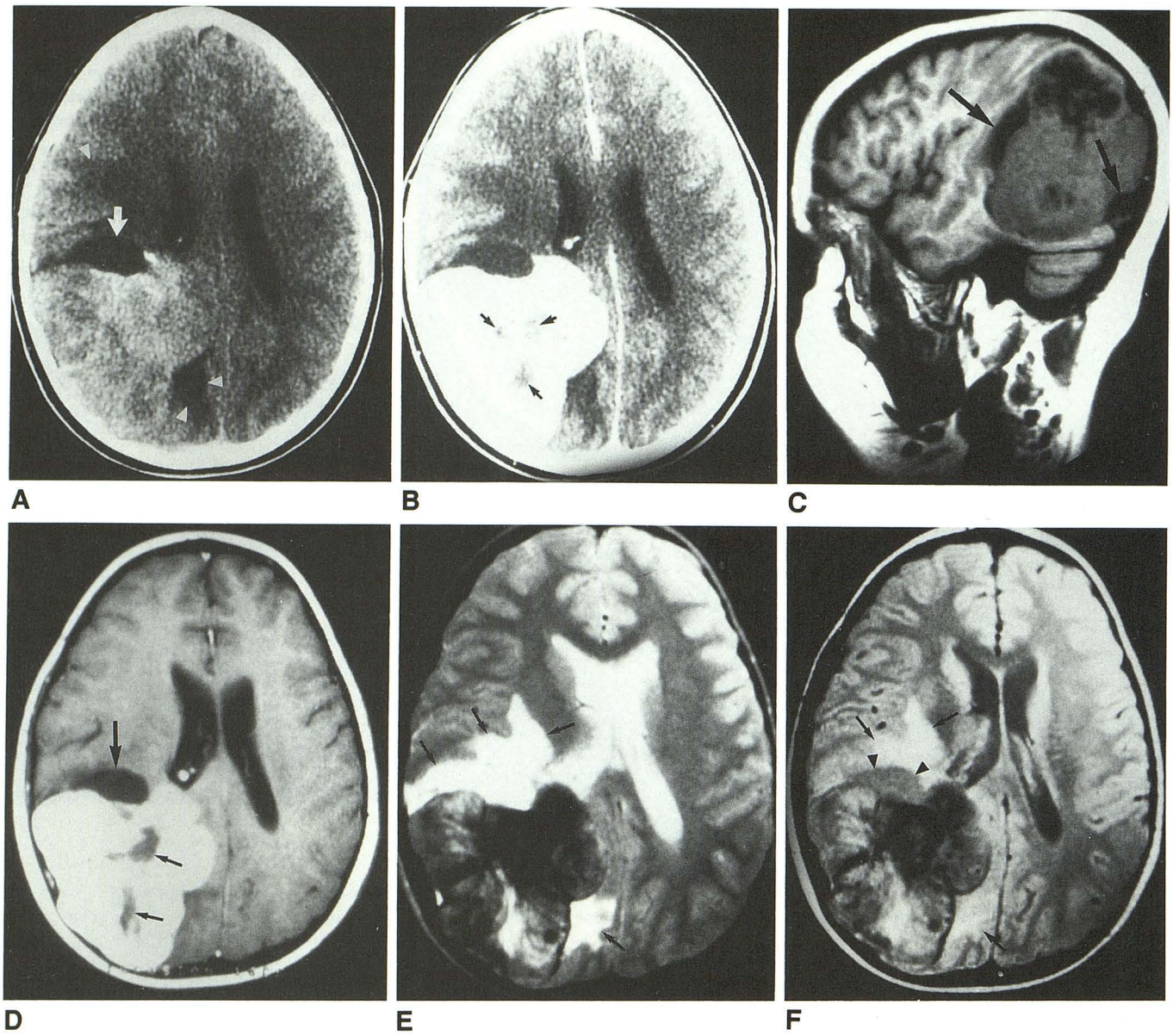

Fig. 6. Fibrous meningioma (Table 1, case 2).

A, Axial noncontrast CT of a heterogeneously dense right occipitoparietal meningioma with peripheral cysts (*arrows*) and edema (*arrowheads*).

B, Axial contrast-enhanced CT shows marked enhancement of the tumor except the more central areas of sclerosis (*arrows*).

C, Sagittal T1-weighted image demonstrates heterogenous tumor signal intensity with peripheral cysts (*arrows*).

D, Axial T1-weighted postcontrast image again shows tumor enhancement except in the sclerosed regions (*small arrows*) and peripheral cysts (*large arrows*).

E, Axial T2-weighted image best demonstrates the extent of tumoral edema (*arrows*).

F, Axial proton-density–weighted image still shows tumor heterogeneity, but now cysts (*arrowheads*) and edema (*arrows*) are better delineated.

Only two of our children had a significant medical history. Two girls had been treated previously for acute lymphoblastic leukemia with high-dose radiation and with chemotherapy to the central nervous system. The girls presented 13 and 15 years later with intracranial meningothelial meningiomas. Childhood radiation-induced neoplasms are rare, with meningiomas and sarcomas being the most common types reported (9–11). Radiation-induced meningiomas in pediatric patients are rare also because of the long time interval between the radiation therapy and

development of the lesions. Typically, the latent period for the presentation of such tumors is 15 to 20 years; however, they may occur as early as 7 years after radiation treatment (9).

Radiation therapy is usually used for treatment of a primary brain neoplasm such as medulloblastoma or acute lymphoblastic leukemia. Meningiomas have been known to occur after both low- and high-dose brain radiation. Malignant lesions are more commonly seen at the higher radiation levels. The majority of radiation-induced meningiomas are benign and behave like non–radiation-induced meningiomas. Histologically, the two are indistinguishable (9–11). Combining the histories of brain radiation with an appropriate latent period, we felt that these two cases did represent radiation-induced meningiomas.

Surgical Pathology

There were no malignant meningiomas in our series. Review of the literature yields different opinions as to whether malignant meningiomas are more prevalent in children. In the older literature, the incidence of malignant meningiomas was 10% in the pediatric population (11). It was later found that some sarcomas of the meninges were incorrectly classified as malignant meningiomas. The most recent literature does not support an increased incidence of malignant meningiomas in children. An incidence of 2% to 5% is cited, approaching that found in the adult population (2, 4, 7, 8, 12).

Cystic meningiomas are typically seen during infancy (13). Only three children in this series had meningiomas with definite cystic components. The solid component of the tumor was larger than the cysts in every case. In order for a meningioma to be defined as cystic, the larger component should be cystic with a negligible to small solid component (13, 14). Also, the older ages of children in this series (4 to 18 years) may account for the absence of large cystic types of meningiomas.

The cysts associated with meningiomas can be classified into four types (14). In type 1, the cyst is located in the center of the tumor; in type 2, it lies at the periphery of the tumor; in type 3, the peripheral cyst extends into the adjacent parenchyma; and in type 4, the cyst lies actually between the meningioma and the brain. It may be possible to determine the type of cyst based on its location using multiple imaging planes with MR.

The medical literature reports a lack of dural attachment as another characteristic finding (28%) in pediatric meningiomas (1). This was not a characteristic in our series: six children had traditional dural-based tumors. Of the two cases of non–dural-based lesions, one child had a typical intraventricular meningioma (Fig 4). Intraventricular meningiomas are observed more commonly in children (16% to 20%), than in adults (0.5% to 4.5%) (15). Meningiomas originating from intraventricular locations, usually the left lateral ventricle, are thought to arise from either the tela choroidea or from the choroid plexus. These meningiomas must be differentiated from other intraventricular lesions such as choroid plexus papilloma, ependymoma, and astrocytoma. MR and CT characteristics along with tumor configurations and ventricular location will assist in ranking the diagnostic possibilities.

The second case of non–dural-based meningioma occurred in an unusual location, arising from deep within the sylvian fissure (Fig 5). There have been several reports of similar lesions in the pediatric literature. It is postulated that these meningiomas arise from arachnoidal capsules originating from pia-arachnoid membranes within the sylvian fissure (16, 17). A meningioma in this particular location may be more difficult to differentiate from other primary intraaxial brain neoplasms such as astrocytomas and some supratentorial ependymomas. Primitive neuroectodermal tumors can, in the majority of cases, easily be distinguished by their markedly heterogenous internal features.

Imaging

An interface between the brain and meningioma has been described and seen best on sagittal T1-weighted images of MR (18–23). The interface is caused by one or more structures including pial vasculature (ie, draining veins), CSF cleft, dural margin, and/or a connective tissue capsule of the meningioma. When the interface is caused by a vascular rim, signal flow void is usually demonstrated on T1-weighted images. Signal intensity may be increased or decreased on either T1-weighted or T2-weighted images depending on whether the structure is arterial or venous and on the flow rate (18, 22). After gadolinium, there may be enhancement of the vascular rim (Fig 3), or signal flow void still may be demonstrated if the flow is very rapid.

An interface may exhibit low signal intensity on T1-weighted and T2-weighted images with enhancement of portions of the interface after contrast material is given. This pattern suggests a fibrocollagenous connective tissue capsule described by Nakasu (22). CSF cleft interfaces follow the usual signal intensity patterns of CSF (Fig 2).

CT was comparable to MR in diagnosing intracranial meningiomas. It came as no surprise that MR proved superior in providing more detailed information regarding the tumor. MR allowed better delineation of the borders of the meningioma, associated edema, interfaces, and cystic areas. Although calcification was not identified readily in the majority of our MR cases, this was not an essential feature.

The MR signal intensity patterns were not predictive of histologic subtype because of similar imaging features. This may become possible in the future with additional reporting of childhood intracranial meningiomas allowing better MR and histologic correlation. MR spectroscopy and other newer techniques may facilitate this correlation.

The diagnosis was made in six of the eight children based on typical location, apparent dural attachment, signal intensity, and enhancement patterns of the solid tumor portion before surgical intervention. These findings did not differ significantly from those of adult intracranial meningiomas, which are well described and documented in the medical literature. In the cases of the intraventricular and deep sylvian fissure meningiomas, the diagnosis was suspected and included in a differential based on similar imaging characteristics despite the more atypical locations.

Conclusions

In our series of eight children with intracranial meningiomas, the tumors exhibited MR characteristics similar to their adult counterparts. The pediatric meningiomas did present more commonly as large lesions (>5 cm), but otherwise a diagnosis can be made based on the classic imaging criteria described in the literature using CT and/or MR.

Acknowledgments

We gratefully acknowledge the dedicated efforts of Ms Sharmaine Ross, Ms Jeannette Wright, Ms Romanita Ross, and Mr Vincent Mahler in the preparation of this manuscript.

References

1. Ferrante L, Acqui M, Artico M, Mastronardi L, Rocchi G, Fortuna A. Cerebral meningiomas in children. *Childs Nerv Syst* 1989;5:83–86
2. Scheithauer BW. Tumors of meninges: proposed modifications of the World Health Organization classification. *Acta Neuropathol* 1990;80:343–354
3. Elster AK, Challa VR, Gilbert TH, et al. Meningiomas: MR and histopathologic features. *Radiology* 1989;170:857–862
4. Drake JM, Hendrick EB, Becker LE, Chuang SH, Hoffman HJ, Humphreys RP. Intracranial meningiomas in children. *Pediatr Neurosci* 1985–86;12:134–139
5. Kolluri VRS, Reddy DR, Naidu MRC, Rao BP, Sumathi C. Meningiomas in childhood. *Childs Nerv Syst* 1987;3:271–273
6. Chan RC, Thompson GB. Intracranial meningiomas in childhood. *Surg Neurol* 1984;21:319–322
7. Davidson GS, Hope JK. Meningeal tumors of childhood. *Cancer* 1989;63:1205–1210
8. Herz DA, Shapiro K, Shulman K. Intracranial meningiomas of infancy, childhood and adolescence. *Childs Brain* 1980;7:43–56
9. Moss DS, Rockswold GL, Chou SN, Yock D, Berger MS. Radiation-induced meningiomas in pediatric patients. *Neurosurgery* 1988;22:4:758–761
10. Balasubramaniam C, Armstrong D, Cheek W, Laurent J. Postradiation meningiomas in a child. *Pediatr Neurosci* 1988;14:319–323
11. Kumar PP, Good RR, Skultety FM, Liebrock LG, Seveson GS. Radiation-induced neoplasms of the brain. *Cancer* 1987;59:1274–1282
12. Alvarez F, Roda JM, Romero MP, Morales C, Sarmiento MA, Blazquez MG. Malignant and atypical meningiomas: a reappraisal of clinical, histological, and computed tomographic features. *Neurosurgery* 1987;28:51–57
13. Katayama Y, Tsubokawa T, Yoshida K. Cystic meningiomas in infancy. *Surg Neurol* 1986;25:43–48
14. Reddy DR, Kolluri VRS, Rao KS, et al. Cystic meningiomas in children. *Childs Nerv Syst* 1986;2:317–319
15. Jelinek J, Smirniotopoulos JG; Parisi JE, Kanzer M. Lateral ventricular neoplasms of the brain: differential diagnosis based on clinical, CT and MR findings. *AJNR Am J Neuroradiol* 1990;11:567–574
16. Cho BK, Wany KC, Chang KH, Chi JG. Deep sylvian meningiomas in a child. *Childs Nerv Syst* 1990;6:228–230
17. Silbergeld D, Berger M, Griffin B. Sylvian fissure meningioma in a child: case report and review of the literature. *Pediatr Neurosci* 1988;14:50–53
18. Atlas SW, ed. *Magnetic resonance imaging of the brain and spine.* New York: Raven, 1991:328–345
19. Edelman RR, Hessel NK Jr. *Clinical magnetic resonance imaging.* Philadelphia: Saunders, 1990:455–458
20. Zimmerman RA, Fleming CA, Saint-Louis LA, Lee BCP, Manning JJ, Deck MDF. Magnetic resonance imaging of meningiomas. *AJNR Am J Neuroradiol* 1985;6:149–157
21. Pomeranz S. *Craniospinal magnetic resonance imaging.* Philadelphia: Saunders, 1989:228–230
22. Nakasu S, Nakasu Y, Matsumura K, Matsuda M, Handa J. Interface between the meningioma and the brain on magnetic resonance imaging. *Surg Neurol* 1990;33:105–116
23. Spagnoli MV, Goldberg HI, Grossman RE, et al. Intracranial meningiomas. *Radiology* 1986;161:369–375